

We are IntechOpen, the world's leading publisher of Open Access books Built by scientists, for scientists

6,900

Open access books available

186,000

International authors and editors

200M

Downloads

Our authors are among the

154

Countries delivered to

TOP 1%

most cited scientists

12.2%

Contributors from top 500 universities



WEB OF SCIENCE™

Selection of our books indexed in the Book Citation Index
in Web of Science™ Core Collection (BKCI)

Interested in publishing with us?
Contact book.department@intechopen.com

Numbers displayed above are based on latest data collected.
For more information visit www.intechopen.com



Laser Opto-Electronic Oscillator and the Modulation of a Laser Emission

Alexander Bortsov

Abstract

The autonomous optoelectronic generator (OEO) is considered in the chapter as a source of low-noise oscillations. Differential equations are considered and methods with OEO modulation with direct and external modulation are analyzed. The complexity of both approaches is related to the non-standard way of description of the nonlinear method modulation for the internal (direct) structure and the utilization of the specific Mach-Zehnder modulator for the first stage on external modulation. The purpose of the presentation is to consider the main features of OEO as a low-noise generator. This includes consideration based on the study of differential equations, the study of transients in OEO, and the calculation of phase noise. It is shown that different types of fibers with low losses at small bending radii can be used as a FOLD in OEO. The important role of the choice of a coherent laser for OEO with a small spectral line width is shown. The prospects of using structured fibers with low losses at bends of less than 10 mm in OEO are described. The results of modeling dynamic processes in OEO with direct modulation are presented.

Keywords: opto-electronic oscillator, phase noise, optical fiber, QW laser, microwave oscillator

1. Introduction. The opto-electronic oscillator structure

Development and creation of the compact ultra-low-noise microwave signal sources, which would be impact-resistant, is an important problem of modern radio-physics and radio engineering. Levels of the phase noise spectral density at the microwave source output must be for most of the applications $-120 \dots -170$ dB/Hz at generation frequency $8 \dots 12$ GHz for 1-kHz offset from a carrier. Constructions of these oscillators must sustain the strong mechanical impact loads in $200 \dots 2000$ N/cm and high accelerations up to $2 \dots 10$ g. Geometrical dimensions of the modern signal sources should often be approximately $10 \times 10 \times 10$ cubic mm, especially for the satellite applications.

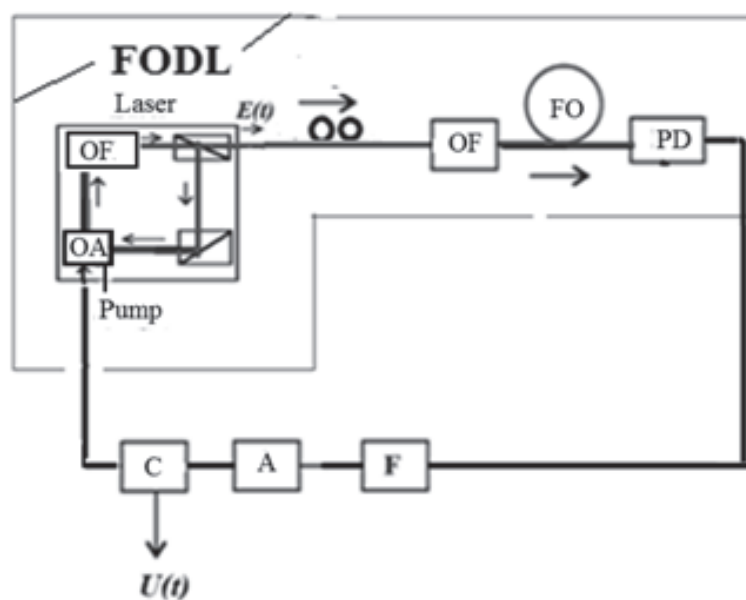
Development and implementation of new compact microwave and millimeter-wave oscillators with improved performance would lead to revolutionary jump in radio electronics, perhaps, comparable to discovery of the quantum-dimensional lasers or (as in radio engineering) at arriving of the high-stability quartz crystal resonator. The new type of oscillators called as opto-electronic oscillator (OEO) described in this paper will permit to use in the mobile communications and in

Internet systems of new radiofrequency channels for information transmission, including 30 ... 75-GHz ranges at the low power of transmitters. A number of publications devoted to OEO experimental investigations grows each year [1–8].

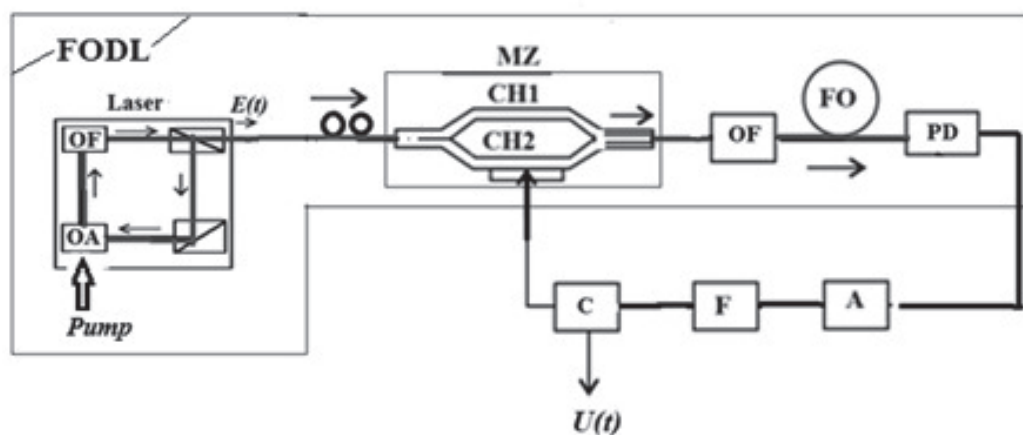
Opto-electronic oscillators will undoubtedly find wide application in the fiber-optical communication lines as well as in on-board radar systems on millimeter- and centimeter ranges, in communication systems as low-noise local oscillators in receivers and as a master clock in transmitters, in an optical lidar technology, as sensors of different physical quantities and in many other systems [8–16].

OEO diagrams with the direct modulation (OEO DM) presented in **Figure 1a** and the OEO structural diagram with *external modulation* of optical emission, which is often called as an opto-electronic oscillator with the Mach-Zehnder modulator (OEO MZ) presented in **Figure 1b**.

Let us consider the case of OEO operation with a small modulation index, and under the condition that the width of the spectral line of the optical laser



(a)



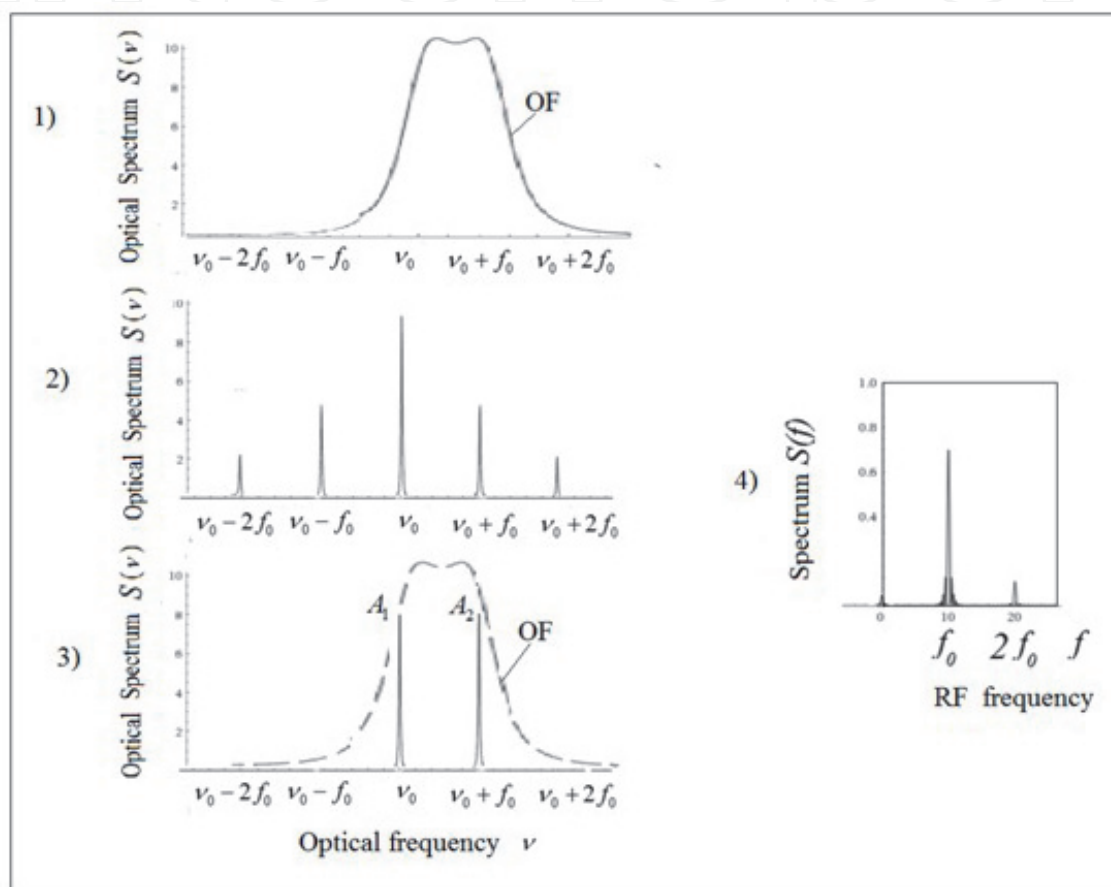
(b)

Figure 1.

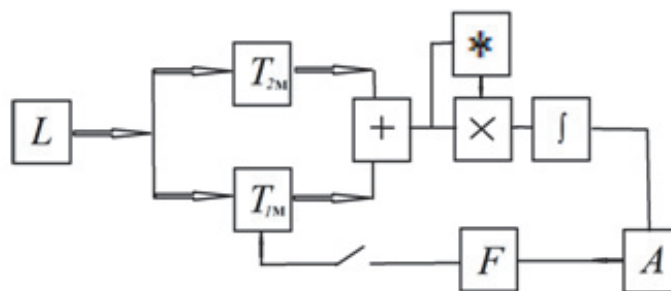
Structural diagrams of the optoelectronic oscillator (a) with the direct modulation by current and (b) with external Mach-Zehnder modulator. Laser = the optical quantum generator (the laser or QWLD), MZ = the electro-optical MZ modulator, OA = the optical amplifier, OF = the optical filter, OF = the optical fiber, P_p = the pumping power, PD = the photo-detector, NA = the nonlinear amplifier, F = the RF filter, C = the RF coupler, CH1, CH2 = the optical channels of the MZ modulator.

generation $\Delta\nu_L$ is much smaller than the radio frequency f_0 of the OEO generation: $\Delta\nu_L \ll f_0$. In this case, the spectrum of the modulated radiation can be represented by several harmonics. We will limit our analysis to the case of two or three optical harmonics, respectively, with frequencies $\nu_1 = \nu_0 - f_0$, $\nu_2 = \nu_0$, $\nu_3 = \nu_0 + f_0$. Two of these optical frequencies ν_1 and ν_2 are spaced from the central optical laser frequency ν_0 by the sub-carrier frequency f_0 .

Figure 2a and **b** shows the analog model of statistical processes in OEO MZ with utilization of the random variables correlator. The correlator structure is described in [16]. It consists of the multiplier “*”, two optical channels with different delays, and the delay cell defining by the delay in the optical fiber. The functional diagram **Figure 2a** and **b** illustrating principles of the correlator method and the frequency



(a)



(b)

Figure 2.

The functional diagram illustrating principles of the correlator method and the frequency discriminator method in OEO with the MZ modulator and in the circuit with direct amplitude modulation at suppression of the one harmonic. a) Diagrams (1–4) of optical frequency selection; b) L = the laser, T_{1M} and T_{2M} = delay lines have delay times in channels, “+” = (adding), “x” = (multiplication), “*” = (conjugate operation), “∫” = (integration), F = the low-pass filter, a = the amplifier.

discriminator method in OEO with the MZ modulator and in the circuit with direct amplitude modulation at suppression of the one harmonic.

2. OEO with direct modulation and OEO with the Mach Zehnder modulator

As in [8–16] when studying noise, OEO is considered here as an optoelectronic system in which oscillations are formed in the optical and radio frequency ranges. The oscillation frequency of the laser is approximately 200 Hz, and the radio frequency of the OAO generation is approximately 10 GHz. A VLD quantum-dimensional laser diode is used to generate laser radiation. The positive feedback ring is formed by an optoelectronic circuit consisting of a modulator, an optical fiber, a photodetector, an electronic amplifier, an electronic filter, and a directional coupler.

Fluctuations are formed at the OEO output. Laser fluctuations are of a quantum nature. When using a low-noise amplifier, the phase fluctuations of the laser determine mainly the noise of the OEO output.

3. OEO construction and its operation principle

Figure 1a shows a direct modulated OEO diagram. At the same time, the QWLD laser it works in the mode of amplitude modulation or intensity modulation. In **Figure 1b** the diagram of the OEO with external modulation is presented.

The OEO DM diagram (**Figure 1a**) is formed by a QWLD laser; a single-mode optical fiber (FO); a photodetector (FD); an electronic amplifier (A); an electronic filter (F), for example, based on a dielectric microwave resonator. The OEO MZ diagram (**Figure 1b**), in addition to the QWLD laser, includes elements that form a closed loop: the Mach Zehnder modulator (MZ); a fiber-optic system (FOS) containing an optical filter (OF) and single-mode optical fiber (FO); photodetector (PD), such as a quantum photodiode size; narrow-band RF filter (F), nonlinear amplifier (A), and directional coupler (C). A fiber-optic delay line (RF FODL) is formed by a laser connected in series, OF, FO, and PD (**Figure 1a**), or by a laser connected in series, MZ, OF, FO, and PD (**Figure 1b**). OEO can be considered as a delayed feedback oscillator.

Figure 1a and **b** show a laser as a source of optical oscillations, which includes a closed-loop optical amplifier (OA) and an optical filter (OF). We consider the case of the laser radiation modulation mode for single-mode, single-frequency, and linearly polarized optical radiation. When self-excitation conditions are met in such OEO systems (**Figure 1**) generation of microwave range oscillations occurs. A fiber-optic delay line (RF FODL) is formed by a laser connected in series, OF, FO, and PD (**Figure 1a**), or by a laser connected in series, MZ, OF, FO, and PD (**Figure 1b**). OEO can be considered as a delayed feedback oscillator.

Figure 1a and **b** shows a laser as a source of optical oscillations, which includes a closed-loop optical amplifier (OA) and an optical filter (OF). The pump or pumping power P_p of the laser is shown conditionally.

We consider the case of the laser radiation modulation mode for single-mode, single-frequency, and linearly polarized optical emission of the highly-coherent laser. When self-excitation conditions are met in such OEO systems, **Figure 1** generation of microwave range oscillations occurs.

In the diagram in **Figure 1**, the Laser is presented by closed into a loop the optical amplifier (OA), the optical filter (OF), which corresponds to the “traveling-

wave” laser or the fiber-optical laser. The optical pump power P_p acts at the active amplifier. If the excitation conditions are met, the laser generates optical oscillations which pass from its output into MZ, then pass via two optical channels with different delays, combine together and through OF and FO acts to the light-sensitive PD area. An effective modulation by MZ is possible in microwave range only for single-mode single-frequency and linear-polarized emission of the highly-coherent laser. Quantum-Well (QW) laser diodes and the fiber-optical lasers with polarizers at their outputs are such emission sources.

The laser is the pump source for the radiofrequency network (**Figure 1b**) closed into a loop and formed by a modulator, an optical fiber, a photo-detector, an electronic amplifier, an electric filter, and a coupler.

As a result of oscillation processes, the spectra are formed with fluctuations having the various nature, but the spectral line width of radiofrequency oscillations is defined by parameters of two oscillating system: the laser and the radiofrequency oscillator.

4. Problem statement

At present, in large-dimension models of laser OEO (**Figure 1**) with the fiber-optical delay line the low phase noise level of -157 dB/Hz [5, 6] is achieved on the 10 GHz generation frequency at 1 kHz offset from a carrier.

Experimental and theoretical investigations of the power spectral density of the laser oscillator phase noise described in [16], show that reduction of the phase noise level of OEO in many respects depends on the laser phase noise level. At oscillation frequency 8 ... 10 GHz at standard offsets from 1 to 10 kHz, the power spectral density of the phase noise is -120 dB/Hz ... -140 dB/Hz.

Appearance on the commercial market of nano-dimension optical fibers with low losses (down to 0.001 dB per one bend, at small bend radii up to 2 ... 5 mm) becomes the stimulus for improvement of OEO radiofrequency generation methods. This allows implementation of comparably small (by geometric linear maximal dimensions) fiber-optical $5\mu\text{s}$ delay lines of 10 ... 30 mm.

In spite of the growth of publications devoted to OEO experimental investigations, the theoretical analysis and systematization of main mechanisms of the phase noise suppression in the low-noise laser OEO was not yet described in known literature. The laser phase noise influence on the OEO radiofrequency phase noise was not researched yet.

The purpose of the presentation is to consider the main features of OEO as a low-noise generator. This includes consideration based on the study of differential equations, the study of transients in OEO, and the calculation of phase noise. It is shown that different types of fibers with low losses at small bending radii can be used as a FOLD in OEO.

Following to an approach described in [16], for OEO noise analysis, we consider the system in **Figure 1**, in which two different oscillation processes are developed: laser oscillations with the generation frequency of approximately 200 THz and 10-GHz oscillations in the radiofrequency network closed into a loop. At that, the frequency multiplicity is approximately 20,000.

5. Laser in OEO

We will assume that the laser in OEO has high coherence and the spectral line width is much smaller than the average generation frequency, and the laser

oscillations can be considered close to sinusoidal, and with a phase component of noise with normalized amplitude noises $m_{Lm}(t)$ and the phase noise component $\varphi_{Lm}(t)$:

$$E_L(t) = [E_{0L} + m_{Lm}(t)] \cos [2\pi\nu_{0L}t + \varphi_{0L} + \varphi_{Lm}(t)]. \quad (1)$$

Here $E_L(t)$, E_{0L} , $m_{Lm}(t)$ are normalized non-dimensional quantities, respectively: the instantaneous intensity, the EMF intensity amplitude, and the EMF amplitude noise, ν_{0L} is the average laser oscillation frequency, φ_{0L} is the initial constant phase shift, t is the current time.

In the opto-electronic oscillator system, under fulfillment of excitation conditions in the electronic part of such an oscillator, the radiofrequency oscillations $u = u_g(t)$ give rise. At that, the radiofrequency signal passes to the electric MZ input from the output of a nonlinear amplifier through the C coupler during oscillation generation. The instantaneous voltage of this signal is

$$u_g(t) = [U_{10MZ} + m_{em}(t)] \cos [2\pi ft + \phi_{0e} + \varphi_{em}(t)], \quad (2)$$

where $U_{0.1MZ} = U_{01C}$ is the amplitude of fundamental oscillation at the electric input of the MZ modulator or at the C output, f is the oscillation radiofrequency, ϕ_{0e} is the constant phase shift, $\varphi_{em}(t)$ are electronic phase fluctuations, $m_{em}(t)$ are electronic amplitude fluctuations.

The low-noise single-mode and single-frequency quantum-dimension laser diodes or the fiber optical lasers are used as the light sources in OEO.

The laser included in the OEO structure (**Figure 1**) is formed by (closed in the loop) the nonlinear OA, the narrowband optical filter (OF), and the optical delay line. The optical oscillation frequency ν_{0L} , which is generated by the quantum-dimension laser diodes in the autonomous steady-state, can be found (under excitation condition fulfillment) on the basis of the phase balance equations solution for the steady-state optical intensity oscillations in the optical resonator and in the laser active element.

To reveal the main mechanisms of the laser noise influence on the OEO radio-frequency noise, the laser can be described by a system of semi-classical equation with the Langevin's sources of the white noise (ξ_E, ξ_P, ξ_N), relatively, for the EMF intensity E_L , a polarization of the laser active material P_n , a population difference N . We studied the laser equation system under its operation in the single-frequency single-mode regime. At that, oscillation are linear-polarized. The main assumption for utilization of semi-classical equations is that the carrier life time on the upper operation level and the time constant T_{OF} of the laser optical filter (OF) are much larger than the relaxation time of polarization T_2 . At that, the equation system with the Langevin's sources for the laser can be written as:

$$\begin{cases} \frac{d^2 E_L}{dt^2} + \frac{1}{T_{OF}} \frac{dE_L}{dt} + (2\pi\nu_{0F})^2 E_L = \frac{2\omega^2 P_n}{\epsilon_n} + \xi_E; \\ \frac{d^2 P_n}{dt^2} + \frac{1}{T_2} \frac{dP_n}{dt} + (2\pi\nu_{12})^2 P_n = \frac{p_e^2}{h} N E_L + \xi_P; \\ \frac{dN}{dt} = \alpha_{N0} \cdot J_{0N} - \frac{N}{T_1} - \frac{1}{h} P_n E_L + \xi_N; \end{cases} \quad (3)$$

In (3) T_2 is the polarization time constant, the excited particles at the upper energy level, T_1 is the lifetime of the excited particles at the upper energy level,

T_{0F} is the time constant of the optical resonator, p_e is the combined dipole moment, h is the Planck constant, ν_{0F} is the natural frequency of the optical resonator on the specific n-th longitudinal mode, ν_{12} is the optical frequency of the transition, J_0 is the constant pump current, $\alpha_{N0} \cdot J_0 = (N_{02} - N_{01}) / (N_{02} T_1)$ is the constant pump, ϵ_n is the permittivity, ν_{0F} is the intrinsic optical frequency of the resonator, P_n is the polarization of the active material, $N = (N_{02} - N_{01})$ is the population difference between the excited and unexcited levels produced by the pumping.

It should be noted that Eqs. (3) are similar to well-studied equations in the oscillator theory for the double-circuit autonomous oscillator with the inertial auto-bias chain with fluctuations.

6. Compact fiber optic delay line in OEO

At first, we would like to note that in RF FODL with geometric length of the optical fiber of 1 ... 5 km, the useful volume (in which emission propagates in the regime of one transverse mode) is not more that one cubic centimeter.

The extremely small geometric dimensions and dimensions of the FODL OEO are important for its use in on-board systems of flying unmanned vehicles, since it is possible to implement effective systems for suppressing force vibrations and accelerations and to make high-precision thermal stabilization systems.

It is comparable in size to other commercial low-noise sources of microwave oscillation. **Figure 3**, and represents a diagram of the maximum sizes for various oscillators that operate in the 10 GHz frequency range: 1 - the quartz resonator (QR), 2 - the disk dielectric resonator from ceramic alloys (DR), 3 - the disk dielectric resonator from leuco-sapphire (DDLS), 4 - OEO the fiber-optical delay line (OEO RF FODL) (delay time is 10–50), 5 - the optical disk microresonator (ODR).

Figure 3, and shows that the smallest dimensions of the resonator have ODR. The dimensions of modern microresonators, taking into account optical input and output devices, lie in the range of about 10...100 cubic microns. **Figure 3b** shows a

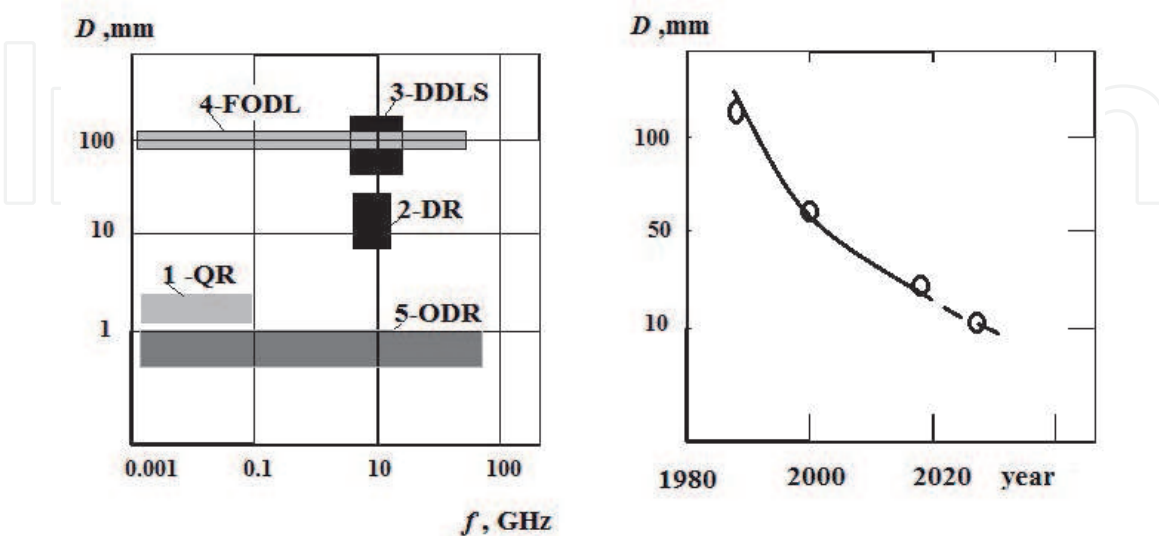


Figure 3. Maximal dimensions of resonators and delay lines used in modern high-stable OEOs and microwave oscillators (a). Dependence of the resonator size in years (delay time is 50 μ s). 1 - QR - The quartz resonator, 2 - DR - The disk dielectric resonator from ceramic alloys, 3 - DDLS - The disk dielectric resonator from leuco-sapphire, 4 - FODL - The fiber-optical delay line (delay time is 10–50 μ s), 5 - ODR - The optical disk resonator. The plot of maximal overall dimensions' variations of the fiber reels in years (b).

graph of the geometric dimensions of the FODL coil of a single-mode optical fiber (the geometric length of the optical fiber is 5...10 km).

The development of microstructural optical fiber technologies with low bending losses suggests that in a few years the maximum geometric dimensions of RF FODL will be 10...50 mm. This becomes possible because microstructured nanofibers have a minimum loss of 0.001 dB per bend at a bending radius of 2...3 mm. It becomes possible to reduce the thickness of the optical shell and reduce the required volume. In this case, it is possible to apply the technology developed by the author [16] for creating fibers by the plasma method when heating the quartz fiber support tube in the temperature range from 1000° C to 19500° C.

The improvement of the technology of heating blanks of nitrogen-doped quartz glass with the help of microwave generators, the automatic movement of plasma columns along the support tubes will lead to the creation of small-sized low-noise OEO with overall dimensions of 0.5 cm³ with a delay of optical oscillation in it of 50 microseconds.

Figure 4 shows images of various RF FODL with the optical fiber length of 10 km used in OEO.

We note (**Figures 3 and 4**) that FODL geometric dimensions for the length of 10 km with the delay 50 μ s is about 100x100x20 (mm³), and dimensions of the optical disk resonator are 100x100x100 (μ m)³. The record small dimensions of FODL and optical disk resonators allow manufacturing of microwave and mm-wave oscillators in the miniature implementation with relatively high characteristics in noises and frequency tuning.

At the present stage, the geometric dimensions of the FORD AO are approximately equal to the resonator made of leucosapphyre. If we talk about using them in oscillators when generating oscillations with a frequency of 10 GHz.

Note the advantage of the linear topology of the fiber optic delay line FODL in contrast to the leuco sapphire crystal. The optical fiber in the FODL is less susceptible to extreme forces, which results in higher mechanical strength. These technical characteristics are very important, since on-board systems are subject to destructive shock effects and accelerations of several g.

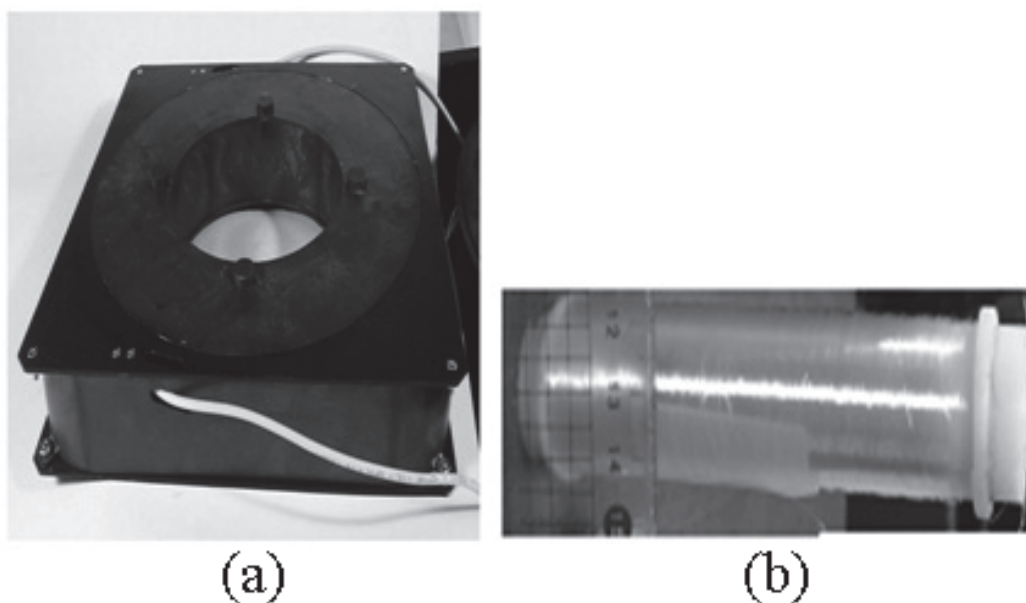


Figure 4. Views of Fiber optic delay line (FODL) with the optical fiber length of 10 km with dimensions 100x100x20 mm³ (a) . View of FODL with optical fiber length of 0.2 km with dimensions 20x 20x100 mm³ (b).

Note that the FODL volume consists of only 10% of optical fiber wound on a quartz cylinder. Therefore, by reducing the critical bend radius when winding the optical fiber and the cladding diameter, it is possible to potentially significantly reduce the maximum dimensions of the FODL OEO.

Moreover, in contrast to the disk microcavity, which is used in synthesizers, the nonlinear optical Kerr effect, FODL in OEO operates in a linear mode. This means that when light passes through an optical fiber, nonlinear effects and additional optical harmonics do not appear. The width of the spectral line of the laser after passing through the optical fiber in the FODL does not change.

Figure 5a and **b** shows profiles of commercial “perforated” optical fibers with the nano-dimension structure of the light-guiding thread.

Note that microstructured fibers with extremely low optical bending losses (**Figure 5**) are used in photonic devices to generate the second optical harmonic. But for this purpose, higher power (more than 20 MW) is used at the input to the single-mode fiber. As a rule, an optical amplifier is placed after the laser or modulator.

Plots of optical losses for different types of optical fibers are shown in **Figure 5a**. From this plot, we can conclude that fibers with HALF type perforation are promising for the development of small-sized delay lines.

Figure 5a shows the dependences of optical losses for different types of optical fibers, and **Figure 5b** shows the cross-sectional profile of a microstructured optical fiber with extremely small losses at small bending radii. Analysis of the research results and optical fibers, gives the right to declare. That the HALF type optical fiber is promising for creating compact FODL [16]. Application of special or nano-dimension optical fibers (**Figure 5**) with low losses at small bend radii (1.3 mm) (0.001 dB/one bend) allows creation of miniature delay lines (1...50 μ s) with overall sizes from 10 to 30 mm [17, 18].

Thus, when using microstructured optical fibers in OEO, it is possible to significantly reduce the dimensions of the fiber-optic delay line of the FODL.

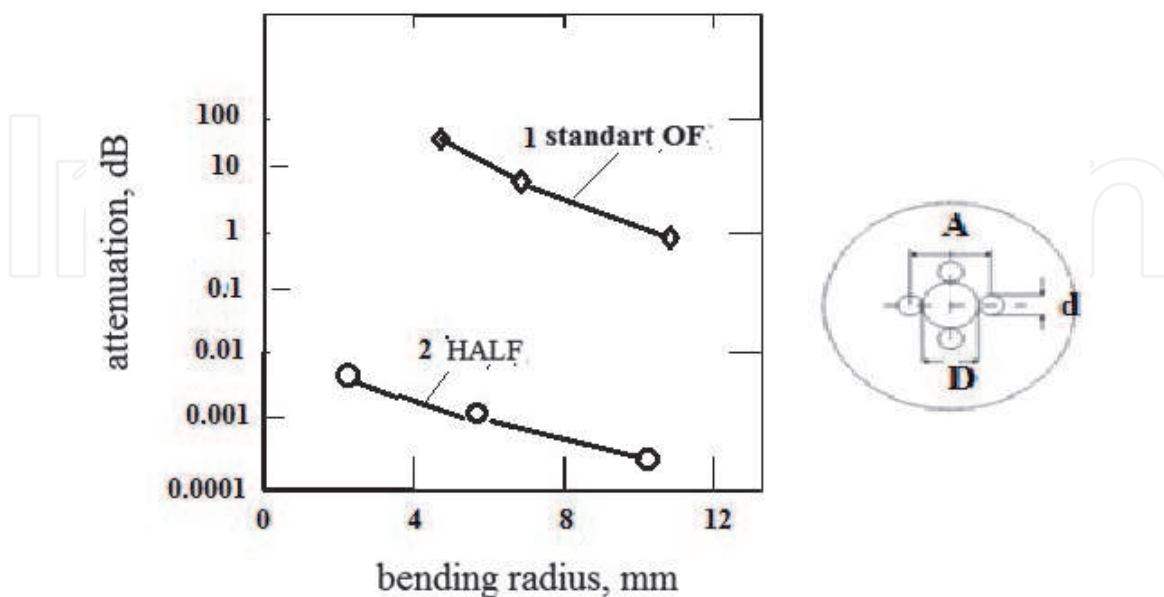


Figure 5.
 a) 1) the plot of bending radius dependencies for standart optical fiber (OF) single-mode fiber G. 652 type with core diameter about 10 microns SMF-28e (corning). 2) the plot of bending radius dependencies for special microstructured optical fiber or hole-assisted light guide fiber (HALF). b) profile of commercial microstructured “perforated” optical fiber with the nano-dimension structure of the light-guiding core.

7. OEO differential equations

To make the differential equations of a closed OEO circuit, it is necessary to keep in mind the following. The positive feedback circuit includes FOS (fiber optic system (FOS), which contains optical filters OF (**Figure 1**) optical amplifier (OA), modulators, photodetector (PD), electronic amplifier(A), electronic filter (F) and couple (C).

Taking into account the remark made, for the transfer function of the “feedback loop” K_{FB} , it is possible to write for the case of OEO DM (**Figure 1a**):

$K_{DL} = K_{FB} = \frac{i_{1L}}{E_n^2} = \frac{J_{1L}}{E_n^2}$, where $E_n = E_L$ is the normalized strength in the QWLD output, which is equal to the value of the FOS input, $i_{1L} = i_m$ is a component of the AC input voltage MZ in the OEM MZ structure and is simultaneously a component of the AC input QWLD in the OEO DM structure. We obtain the following symbolic equation for the variable component of the current:

$$J_{1L} = \frac{[\cos(\Delta\phi_{OF})]|E_n|^2(1/T_{EF})K_{OF}K_{PD}p \exp(-pT_{DL})S_{NY}(J_{1L})}{[p^2 + (1/T_{EF})p + (2\pi f_{0e})^2]}. \quad (4)$$

Taking into consideration the circuit of positive FB, we transfer to equation system in the time domain for OEO DM [16]:

$$\begin{cases} dE_{0L}^2/dt = G_0 \cdot E_{0L}^2 \cdot N_L - E_{0L}^2/T_{OF} \\ dN_L/dt = \alpha_{N00} \cdot J_{0L} + \alpha_{N01} \cdot J_{1L} - \frac{N_{0L}}{T_1} - G_0 N_L E_{0L}^2, \\ d\varphi/dt = 2\pi\nu_{0P}(N_L) - 2\pi\nu_0 + \sigma_{0L} + \rho_{0L}E_{0L}^2, \\ \frac{d^2J_{1L}}{dt^2} + \frac{1}{T_F} \frac{dJ_{1L}}{dt} + (2\pi f_{eF_0})^2 J_{1L} = S_{NY} [E_{0L}^2 K_{FOS} K_{PD}, J_{1L}(t - T_{DL})] \frac{dJ_{1L}(t - T_{DL})}{dt^2}, \end{cases} \quad (5)$$

where the transfer function $K_{DL} = K_{FOS}K_{PD}$, K_{FOS} is the transfer function of FOS, which contains the optical fiber of two fibers of different length, K_{PD} is the transfer function of the photo-detector, which were defined in Chapter 2 in book [16].

Now we present for comparison the similar to (4.18) system from four time-equation for OEO MZ with QWLD [16]:

$$\begin{cases} dE_{0L}^2/dt = G_0 E_{0L}^2 N_L - E_{0L}^2/T_{OF}, \\ dN_L/dt = \alpha_{N00} \cdot J_{0L} - \frac{N_L}{T_{1L}} - G_0 N_L E_{0L}^2, \\ d\varphi/dt = 2\pi\nu_{0P}(N_L) - 2\pi\nu_0 + \sigma_{0L} + \rho_{0L}E_{0L}^2, \\ \frac{d^2U}{dt^2} + \frac{1}{T_F} \frac{dU}{dt} + (2\pi f_{eF_0})^2 U = S_{NY} [E_{0L}^2 K_{MZ} K_{FOS} K_{PD} \cdot U(t - T_{FOLD})] \frac{dU(t - T_{FOLD})}{dt^2}. \end{cases} \quad (6)$$

8. Dynamics of transients in OEO DM

Let us consider the transient process of the exit to the steady-state mode of the free generation of OEO DM at representation of the oscillator in **Figure 1a**. As it had

been mentioned earlier, such a structure is described by the system of differential Eqs. (5). Let us describe in more detail the results of the study of the system of differential Eqs. (5) for OOO DM (**Figure 1a**).

On the base of mentioned OEO differential Eqs. (5), the analog model of OEO was constructed presented in **Figure 1a**.

Figure 5 presents the obtained solutions of system (5) and shows plots of the square of the intensity, population, and pump current, as well as phase portraits in the transient mode under the influence of a constant pump current in the form of a step pulse.

The one of difficulties at solution of (4) finding at the analog modeling is the determination of the nonlinearity of the RF nonlinear amplifier (A) in order to “compensate of the multiplicative QWLD nonlinearity”.

At the same time, in the analog models, the following laser parameters were taken in solution (5) (the same as in Chapter 3 [16]): for the mesa-strip laser with the thickness of the dielectric film $d = 1.2 \mu\text{m}$: $g_0 = 10^3$, $\tau_D = 7,2 \cdot 10^{-12} \text{ s}$, $I_{\text{thr}} = 12 \text{ mA}$, $\epsilon_{sh} = 0$. The values of parameters of QWLD are: the life time of carriers $T_1 = \tau_{n1} = 0.5 \cdot 10^{-9} \text{ s}$, the threshold level population difference is 10^{18} 1/cm^3 , the life time of photons or the time constant of the optical resonator $T_{0F} = \tau_{ph} = 1,2 \cdot 10^{-12} \text{ s}$, the volume of the QWLD active zone is 10^{-11} cm^{-3} .

The modes with and without delay in the OEO feedback ring were investigated. (**Figure 6**).

The pulsations of the square of the intensity and population of the laser in the simulation of the transition process OOO DM are established. These dependences are shown in **Figure 6**. The nonlinear distortions are related to the multiplicative nonlinearity of the laser. And their level depends on the value of the DC pump current of the laser.

The period of laser pulsations in transients, which is approximately 0.4 ns, depends on the level of the pump current and is determined by the carrier lifetime.

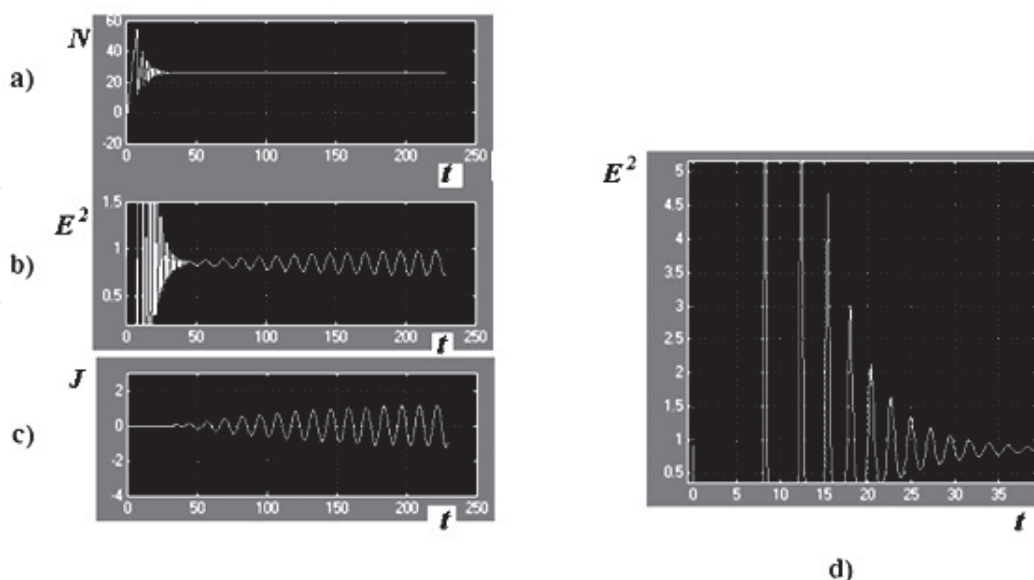


Figure 6.

The transient process in OEO and in the laser. The constant pumping level $J_0 = 30 \text{ mA}$. Activation of pumping occurs in the time moment $t = 0$. Time-functions of normalized values: a) the population difference N (10^{18} 1/cm^3), b) the normalized square of strength $(E)^2 = (E_{oL})^2$, (1.0 point = 1 mW), c) AC component of pumping current, d) the normalized square of strength $(E)^2 = (E_{oL})^2$, (1 point = 1 mW) at initial part [0,50]. The transient process is presented with the exit to the limit cycle on the time diagram E_{oL} , N_o . The scale on the time axis t : 5 points = 0,1 ns. The setting time for the laser oscillations is 40 points (or 0,8 ns). The setting time of OEO RF oscillations is on the time axis t 50 ... 250 points (or 40 ns).

The setting time of the laser oscillations is 0.8 ns (or from 0 to 40 points in **Figure 6a** and **b**). The time of setting the RF oscillations of the OEO on the time axis t is 40 ns (or from 50 to 100 points in **Figure 6**). The oscillation frequency in the steady-state mode is close to the natural frequency of the electronic filter (F) and was approximately 10 GHz.

9. OEO DM system of the laser emission

As follows from the theory of oscillations, in a transient process, a special or critical point can be a stable node, with real and negative roots p_1 and p_2 of the characteristic equation of the system of differential Eqs. (5). When the feedback coefficient in the OEO ring increases, the special point A becomes unstable. In this case, the characteristic roots p_1 and p_2 must be positive.

As shown in **Figure 7**, there is a stable limit cycle around the unstable point A . The generation is impossible if the isoclinic lines $F_1(N_L)$ and $F_2(E_L)$ are not intercepted.

The process of establishing the laser radiation oscillation ends, and then, due to the positive feedback in the OEO DM ring, there are increasing oscillations of the laser charge current, which also modulate the inverse population of the laser. This leads to subsequent oscillations of the square of the electromagnetic field strength of the laser.

If there is a single singular point A in the upper half-plane (**Figure 7**) the condition of self-excitation of the laser is fulfilled. Therefore, the excitation of the OEO DM occurs in a gentle way. This is also true for the case of an arbitrary odd numbers of nontrivial singular points. OEO DM generation may not be possible if the isoclinic lines and are not intersect (**Figure 7**). If the number of singular points is even (if there are two singular points), the condition of self-excitation of the OEO may not be met.

Laser generation can only be excited in a “hard” way, which is initiated by a pulse from an external source.

If we consider the case of an unstable point A , the oscillatory system develops a process of oscillation growth. The nonlinearity of the electronic amplifier limits the growth of oscillations and the conditions for the existence of a limit or closed stable cycle are met (**Figure 7b**).

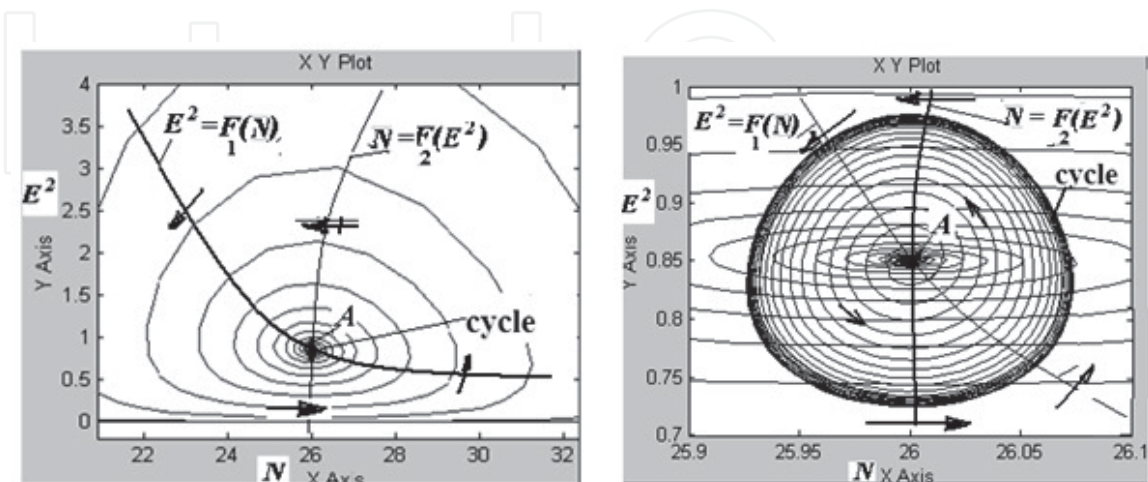


Figure 7. Transition mode scenario in OEO DM. A phase portrait of the normalized square force is presented. a) the phase portrait of the normalized square strength $(E)^2 = (E_{oL})^2$ and the population difference N and . Y-axis – The normalized square strength (or the intensity), X-axis – The population. The scale on the Y axis is $1.0 = 1$ $(V/m)^2$. The scale on the X axis is $1.0 = 1$ mW. N (1.0 point on the scale is 10^{18} $1/cm^3$). b) the enlarged image of the phase portrait is shown and the transient development with the exit to the limit cycle on the time diagram E_{oL} , N_o . The scale on the time axis t is 5 points = 0,1 ns.

If we consider the question the stability of a given oscillation cycle, then its existence is determined by the sign of the partial derivatives of the right-hand sides with respect to one variable when analyzing the characteristic equation obtained in [16], Chapter 4.

The limit cycle is stable only if the corresponding expressions for the coefficients are greater than zero [16].

When considering the hard-excited OEO DM mode, it is necessary to note more complex dynamics, and the picture of the phase plane in the transition mode becomes diverse. The number of singular points (intersection points of isoclinic lines) becomes even. Therefore, long-term generation of OEO DM oscillations in hard mode is possible only when an external generator is operating.

The transients of the oscillation tuning in the OEO DM with no lag in the positive feedback loop are shown in **Figure 8**.

Modeling has shown that strong nonlinear distortions caused by the multiplicative nonlinearity of the laser occur at a large oscillation amplitude [16] and their level is determined by the choice of the operating point or the direct pump current of the laser.

For example, a level of 1 ... 10% of the maximum possible values is performed when a constant bias current is selected at a level of 1.5 to 5.0 exceeding the threshold laser pump current. It is established that the nature of the transient process is determined by the type of non-linearity of the electronic amplifier, the

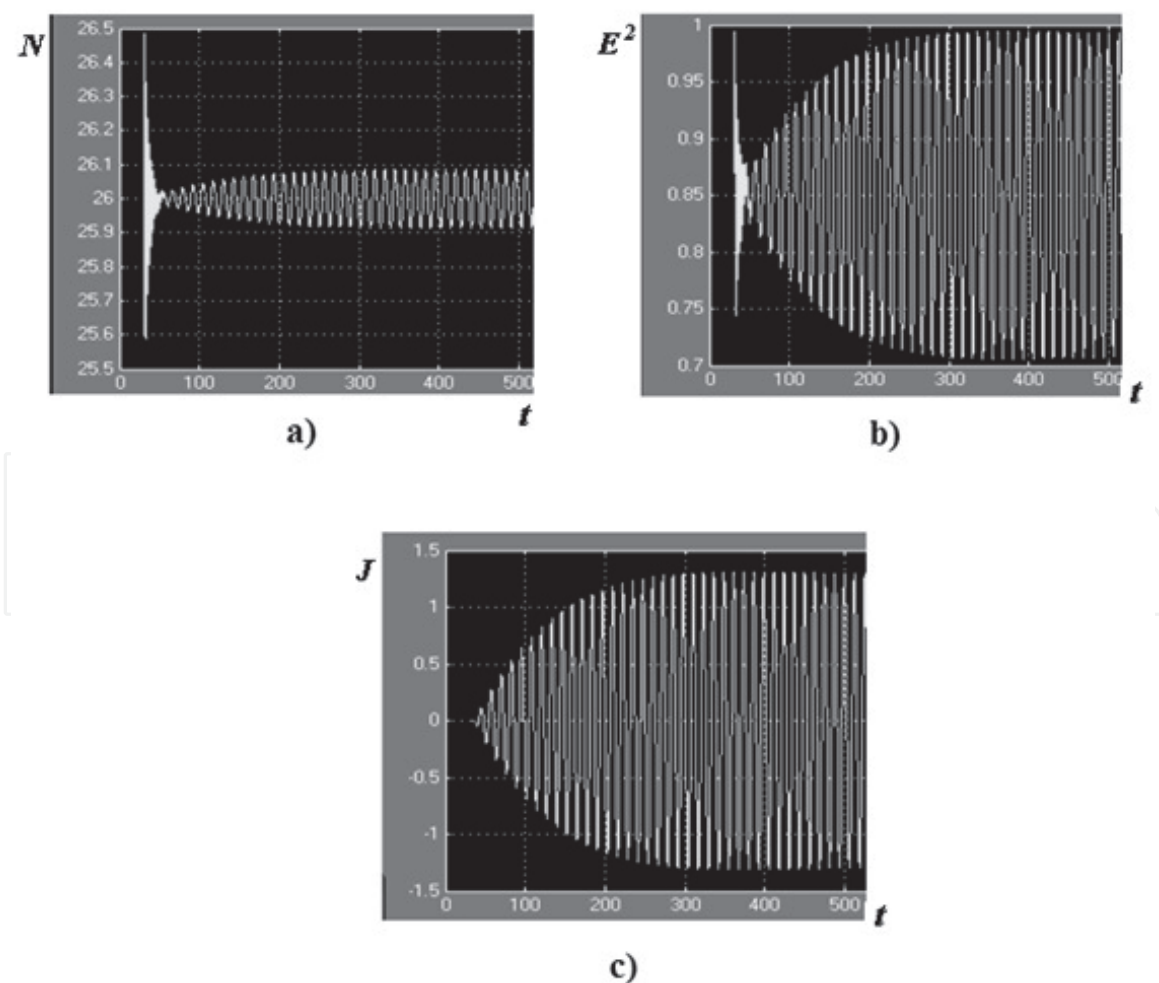


Figure 8. Plots of function of the dependences of the square of the electromagnetic field strength of the laser in the optical channel, the population of carriers and the pump current. In abscissa axis – The normalized time, in ordinate axis – a) N – The inversed population; b) $(E)^2 = (E_{oL})^2$ - intensity of laser; c), – Oscillations of OEO the electrical current of laser pumping.

selection of the natural frequency of the electronic filter, and the delay value in the FODL. At the same time, the duration of the OEO DM oscillation transition process changes significantly.

Positive feedback is included in the DE system, taking into account the photodetection of optical radiation, selectivity in the radio frequency, and nonlinear gain on a nonlinear amplifier.

What is new in the analysis of the OEO DM operation is that the Lotka-Volterra laser differential equations for the optical field intensity, inverted population, and optical phase with positive selective feedback with a delayed argument can be reduced to a single van der Pol differential equation for the pump electric current.

From our studies of differential Eqs. (5), it follows that in OEO DM, single-frequency and two-frequency modes of relaxation oscillations are possible.

For a stable single-frequency mode of OEO DM generation, the following conditions must be met: a twofold excess of the electron filter time constant (F) over the electron relaxation time constant in the active layer of the laser.

10. Laser phase noise and OEO phase noise

Expressions for SSB PSD of the laser phase noise do not reflect the important property of the laser oscillating system: a presence of the relaxation resonance on the frequency ν_{00L} at the offset from a carrier ν_{0L} , i.e., at $F_{00L} = 2\pi(\nu_{00L} - \nu_{0L})$. We can take this “resonance peak” into account at linearization of system [16] with account of the population equation. At that, the expression for SSB PSD of the laser phase noise take a form:

$$S_{PL}/P_{0L} \approx \frac{S_{SL\text{Im}}}{(FT_{0F})^2} + \frac{S_{LE}D_{11}^2 + S_{LN}D_{22}^2}{T_1^4 \left((F^2 - F_{00L}^2)^2 + (F\alpha_{00l})^2 \right)^2} \quad (7)$$

where $F_{00L} = (1/T_1)((T_{0F}/T_1)\alpha_0 - 1)^{1/2}$, α_0 is an excess of DC laser pumping over its threshold value, α_{00l} is a damping decrement, T_1 is the lifetime of the excited particles at the upper energy level, D_{11} and D_{22} are the constant coefficients, and S_{LE}, S_{LN} are relatively, spectral densities of impacts in [15, 16] the Langevinian noise of the laser ξ_E, ξ_N , relatively. Here ξ_E is the noise of the EMF intensity E_L , ξ_N is the noise of a population difference N . **Figure 9** shows the curve 1 of SSB PSD of the

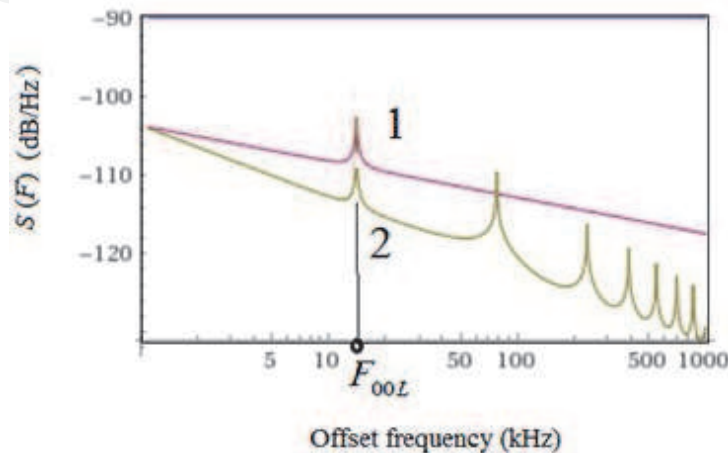


Figure 9. Laser phase noise SSB PSD (curve 1), and OEO phase noise SSB PSD (curve 2).

laser phase noise calculated by formula (7) for $S_{SL\text{Im}} \approx S_{LE} D_{11}^2 S_{LN} D_{22}^2 \approx -105\text{dB/Hz}$, $F_{00L} \approx 14\text{kHz}$, the time constant of the laser resonator $T_{OF} = 10^{-7}\text{s}$.

11. OEO as the EMF correlator

We studied OEO as a correlator of two random variables ξ_1, ξ_2 with probability density at the input of the correlator $p_1(\xi_1, \xi_2)$. The random variables in the extraction of two optical harmonics [16] are phase noise $\xi_1 = \varphi_{10Lm}(t)$ and $\xi_2 = \varphi_{20Lm}(t)$ corresponding harmonics with the amplitudes $A_1 E_{0L}$ and $A_2 E_{0L}$. The resulting phase noise of the current in the load of the PD photodetector is the result of statistical averaging. The distribution probability $p_2(\eta)$ determines the appropriate correlation function of the output process. Where $f(\eta)$ is the nonlinear characteristic of the photo-detector, $\eta_\tau = \eta(t - \tau)$ of the $\eta(t)$ process in the correlator output. At that, $p_1(\xi_1, \xi_2)$ defines the probability density $p_2(\eta)$ of the statistical process in the correlator output (**Figure 2**) of the OEO MZ (**Figure 1b**) at the *closed loop* of OEO MZ for $\tau > T_{FOS}$.

The spectral density of radio frequency OEO oscillations $S_{RFL}(F)$ is determined by the formula:

$$S_{RFL}(F) = \frac{E_{0L}^4}{2} \frac{U_{10MZ}^2 S_L}{2} K_{\Gamma PN}^2 \cdot \left[1 - \frac{A_2}{A_1} \exp\left(-\frac{2(\Delta T_M + T_{FOS})}{T_c}\right) \right], \quad (8)$$

where S_{PL} - SSB PSD of the laser phase noise (7), $K_{\Gamma PN}^2$ is the coefficient of the noise suppression, which depends upon T_{FOS} , the laser optical power E_{0L}^2 , the transfer function of FODL $|K_{FODL}|$, U_{10MZ}^2 is the square of the AC amplitude in the MZ electrical input. When considering OEO as a correlator of two random variables ξ_1, ξ_2 with a probability distribution density at its input $p_1(\xi_1, \xi_2)$, we can conclude from (8) that the SSB PSD of the laser phase noise is significantly determined by the ratio of the delay time in FOS and the laser coherence time, and it significantly depends on the ratio harmonics amplitudes A_2/A_1 .

12. OEO phase noise

From Eqs. (7) with account for nonlinear characteristic of the amplifier A (**Figure 1a**) as a cubic polynomial $i_A(u) = \alpha_{e0}u - \beta_{e0}u^3$ (where u is the instantaneous voltage at the amplifier input, and the average slope of this characteristics is $\sigma_U = \sigma_{e00} - (3/4)\beta_{e00}P_{0G}$) and we can obtain through laser and delay line parameters the power of the Opto-Electronic oscillator radiofrequency generation P_{0G} :

$$P_{0G} = \frac{\alpha_{e00}}{\beta_{e00}} \left(1 - \frac{1}{P_{0L}|K_{FOLD}|\alpha_{e00}\beta_{e00}} \right). \quad (9)$$

We introduce the designation: $Y_{00}/P_{0L} = y_M[1 + FT_{EF}]/|K_{FODL}|$, where y_M is the input normalized conductivity of the MZ modulator. Similarly to (7) for laser PSD, we obtain from the general symbolic Equations [16] the equation for SSB PSD S_Ψ of the OEO phase noise.

SSB PSD S_Ψ reduced to the radiofrequency oscillation power P_{0G} is determined by expression derived in [14–16] according to the Evtianov-Kuleshov approach.

The $K_{\Gamma PN2}^2$ coefficient depends on the delay time in the optical fiber and on the laser optical power and it is equal

$$K_{\Gamma PN}^2 = \frac{\{(Y_{00}/P_{0L})[\sqrt{2} \sin(\pi/4 - FT_{FOS})] - \sigma_U\}^2}{\left\{[(Y_{00}/P_{0L})]^2 - (Y_{00}/P_{0L}) \cdot (1 + \sigma_U) \cos[FT_{FOS}] + \sigma_U\right\}^2} \quad (10)$$

where y_M is the input normalized conductivity of the MZ modulator. Then the function of OEO phase noise PSD can be represented [14–16] as

$$S(F) = \frac{S_{\Psi}}{P_{0G}} = \frac{K_{\Gamma PN}^2 C_A h \nu N_{sp}}{P_{0G}}, \quad (11)$$

where C_A - the constant coefficient, N_{sp} is a number of spontaneous photons received by PD.

Plots of (10) are shown in **Figure 9**, which are limited functions of OEO of the phase noise PSD with account of small noises of PD and the A amplifier, at laser phase noise for the offset frequency 1 kHz equaled to about -120 dB/Hz, at laser power 30 mW, the delay of $T_{BC} = 5 \cdot 10^{-6}$ s (the OF length is 1000 m), $\sigma_U = 1$. We see that the first peak is defined by the laser phase noise PSD, and average suppression of the phase noise for 50 kHz offset is more, that -10 dB/Hz.

It should be noted that at the optical fiber length of 2 km the uniform suppression of the laser phase noise is achieved in the offset range 1 ... 50 kHz.

Calculation of the phase noise suppression factor $K_2(F)$ suppression factor according to (9) is presented in **Figure 10** $\sigma_U = 1$; $\sigma_U = 1$; $T_{FOS}/T_F = 1$, $P_{0L}|K_{FODL}| = 2$ (curve 1); $T_{FOS}/T_F = 10$, $P_{0L}|K_{FODL}| = 2$ (curve 2); $T_{FOS}/T_F = 10$, $P_{0L}|K_{FODL}| = 4$ (3 curve). It can be seen that increase of delay time from $T_{FOS}/T_F = 1$ (curve 1) to $T_{FOS}/T_F = 10$ (curve 2) results in reduction of K_2 factor more than 10 times in the rated offset frequency $F \cdot T_F$ range 0.05 ... 0.5.

It is shown that at OF length, the further reduction of the OEO phase noise is possible using the PLL (phase-locked loop) system. Calculation results are well-agreed with experimental dependences of OEO phase noise PSD, which can be found in [14–16]. Here, we should remind that first publications on research of frequency stability in OEO with the help of FOLD were fulfilled in 1987–1989 at

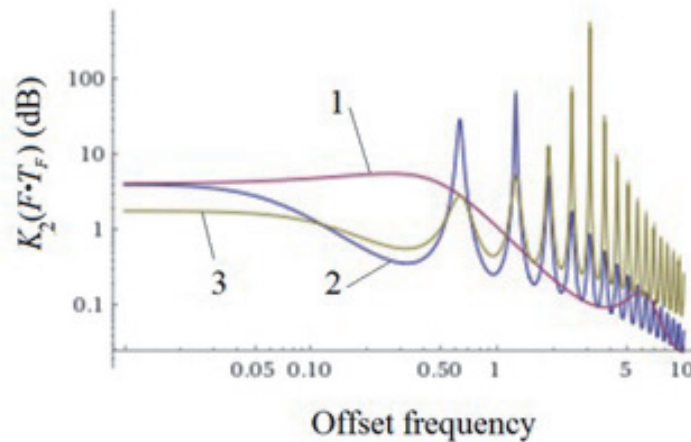


Figure 10.

The phase noise suppression factor $K_2 = K_{\Gamma PN}^2$ (9) versus the rated offset frequency $F \cdot T_F$: $T_{FOS}/T_F = 1$, $P_{0L}|K_{FODL}| = 2$, (curve 1); $T_{FOS}/T_F = 10$, $P_{0L}|K_{FODL}| = 2$ (curve 2); $T_{FOS}/T_F = 10$, $P_{0L}|K_{FODL}| = 4$ (3 curve).

Radio Transmitter Dept. of Moscow Power Engineering Institute (now NRU MPEI) while the OEO circuit was offered in [12, 13].

13. Experimental investigations

Experimental researches were devoted for several experimental OEO of microwave range with various pumping laser diodes, which emit at wavelengths of 1310 nm or 1550 nm. The maximal output power of optical emission for used laser diodes formed about 10 ... 20 mW. **Figure 11** shows the photo picture of one piece assembled on the base of the circuit in **Figure 1b**. As the photo-detector, we applied the PD on the base of InGaAs. The radiofrequency filter represented the dielectric resonator of microwave range with the loaded Q-factor of 1000. This resonator was made on ceramics and had a natural frequency 8.2 GHz. This breadboard model used the wideband (up to 12 GHz) modulation of laser emission, which was performed by the Mach-Zehnder modulator from Hitachi Co. The single-mode light guiders with lengths from 60 m to 4640 m were used for experiments. The stable generation of single-frequency oscillation at frequency close to 8.2 GHz was observed in OEO system for various OF lengths.

The delay of OEO signal was performed with the help of additional fiber-optical light guider with the 10 km-length and the additional photo-diode. The phase noise level at usage of different lasers formed the value $-100 \dots -127$ dB/Hz, for offsets 1 ... 10 kHz from the microwave sub-carrier frequency under generation and it depends on the spectral line width of laser emission.

Essential reduction of the phase noise by 15 dB was observed in OEO using the differential delay line on the base of two optical fibers of different length. These experimental functions are well-agreed with theoretical at account of the stabilization effect at OF lengths more than 2000 m.

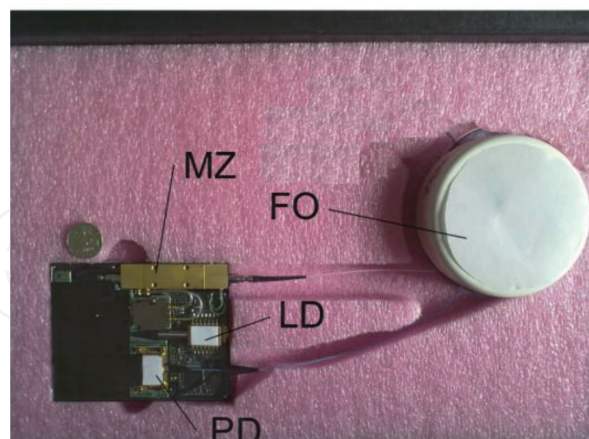


Figure 11.
General view of the experimental breadboard of low-noise laser opto-electronic oscillator of microwave range. The mean oscillation frequency is 8 ... 10 GHz.

14. Conclusion

At that, formation of the final phase RF noises of OEO is examined as the result of the convolution operation of the laser optical spectrum and the RF spectrum of the oscillation. Thus, when using microstructured optical fibers in OEO, it is possible to significantly reduce the dimensions of the fiber-optic delay line -FODL.

For a stable mode of OEO generation in the single-frequency mode, it is necessary to double the time constant of the electron filter (F) over the time constant of the relaxation of electrons in the active layer of the laser.

We have shown that the resonant curve of the electron-photon resonance of the laser has a significant influence on the formation of the power spectral density PSD of the phase noise in OEO. For stable operation of the OEO, the laser coherence time and the delay time in the optical fiber must be balanced. The use of microstructured fibers with low bending losses makes it possible to create compact fiber-optic delay lines for OEO.

Under assumption of the small and large oscillation amplitude at the modulator electrical input, we study OEO as a system in which two oscillation processes are developed on the optical frequency and in radiofrequency. The relatively simple expressions for phase noise PSD of the radiofrequency generation in optoelectronic generator in the mode with the single-side carrier with an account of the laser phase noise. The analysis fulfilled shows that under condition of predominance of laser noises being detected over v noises of the electronic amplifier and the OEO photo-detector of the filtering system.

For reduction of spurious influence of DC intensity component on the photo-detector we offer to use the modulator operation mode with an offset of the optical channels “pi”.

The suppression factor of the OEO laser phase noise at optical fiber lengths from 2 to 10 km is about $-8 \dots -10$ dB/Hz at offset of $F = 1$ kHz. Utilization in OEO of the highly-coherent laser with the phase noise less than $S(F) = -100$ dB/Hz (at the same offset) is the condition of OEO small phase noises less than $S(F) = -130$ dB/Hz at the $F = 1$ kHz offset. The value of the OEO power spectral density is proportional to the spectral line width of the laser optical emission.

Acknowledgements

Authors express our thanks to PhD Yu. B. Il'in for manifested interest and participation in discussions.

IntechOpen

Author details

Alexander Bortsov
NRU MPEI, Moscow, Russia

*Address all correspondence to: laseroe5@gmail.com

IntechOpen

© 2021 The Author(s). Licensee IntechOpen. This chapter is distributed under the terms of the Creative Commons Attribution License (<http://creativecommons.org/licenses/by/3.0>), which permits unrestricted use, distribution, and reproduction in any medium, provided the original work is properly cited. 

References

- [1] Aliou Ly, Vincent Auroux, Ramin Khayatizadeh «Highly Spectrally Pure 90-GHz Signal Synthesis Using a Coupled Optoelectronic Oscillator», *IEEE Photonics Technology Letters*, vol.30,no.14, pp.1313-1316, 2018.
- [2] Dan Zhu, Tianhua Du, Shilong Pan «A Coupled Optoelectronic Oscillator with Performance Improved by Enhanced Spatial Hole Burning in an Erbium-doped Fiber», *Journal of Lightwave Technology*, pp.3726-3732,(2018).
- [3] Zhuansun Xiaobo and etc, «Low phase noise frequency-multiplied optoelectronic oscillator using a dual-parallel Mach–Zehnder modulator», *Optical Engineering* 57(08),p.086101, (2018).
- [4] A. Banerjee et al., «Study of Mutual Injection-Pulling Between Two Mutually-coupled Single-loop Optoelectronic Oscillators», *Optik*, 11 February 2021, pp.166492-166499, (2021).
- [5] A. G. Correa-Mena and etc «Performance Evaluation of an Optoelectronic Oscillator Based on a Band-Pass Microwave Photonic Filter Architecture », *Radioengineering*, 26 (3),pp.642-646,(2017).
- [6] C. X. Li et al., «A Novel Optoelectronic Oscillator with Series-Coupled Double Recirculating Delay Lines», *Advanced Materials Research*, Vols. 986-987, pp. 1730-1733, (2014).
- [7] Xihua Zou, Xinkai Liu, et al., « Optoelectronic Oscillators (OEOs) to Sensing, Measurement, and Detection», *IEEE Journal of Quantum Electronics* 52 (1):0601116, (2016).
- [8] X. S. Yao and L. Maleki, «Optoelectronic microwave oscillator», *J. Opt.Soc. Amer. B, Opt. Phys.*, vol. 13, no. 8, pp. 1725–1735, (1996).
- [9] A. A. Savchenkov, A. B. Matsko, V. S. Ilchenko, and L. Maleki, ” «Optical resonators with ten million finesse», *Opt. Express* 15, 6768-6773 (2007).
- [10] C.W. Nelson et al. «Microwave optoelectronic oscillator with optical gain», *IEEE*, №12,v. 31,pp.152-157, (2007).
- [11] J. J. McFerran, E. N. Ivanov, A. Bartels, G. Wilpers, C. W. Oates, S. A. Diddams, and Hollberg, ” «Low-noise synthesis of microwave signals from an optical source»,” *Electron. Lett.* 41, pp. 650-651 (2005).
- [12] A. A. Bortsov, V. V. Grigoriantz, Yu. B. Il'in « Effect of the lightguide excitation efficiency on the frequency of a self-excited oscillator with a differential fiber optic delay line », *Telecommunications and Radio Engineering*, 44(8), August, 1989, pp. 137-142. (1989).
- [13] V.V. Grigor'yants, Yu.B. Il'in, «Laser optical fibre heterodyne interferometer with frequency indicating of the phase shift of a light signal in an optical waveguide», *Quantum and Quantum Electronics*,21 (5),pp.423-427,(1989).
- [14] Bortsov, A. A. , S. M. Smolskiy «Opto-Electronic Oscillator with Mach-Zehnder Modulator», *Infocommunications Journal*, Vol. XI, No 1, March, pp. 45-53, (2019). DOI: 10.13140/RG.2.2.20992.69126.
- [15] Alexander . A. Bortsov , Sergey M. Smolskiy «Optoelectronic oscillator as the time correlator with ultralow phase noise» , *Opt. Eng.* 59(6) 061618 , 3 February, (2020). DOI: 10.1117/1.OE.59.6.061618.
- [16] Alexander.A. Bortsov, Yuri B.Il'in, Sergey M. Smolskiy «Laser Optoelectronic Oscillators» Springer

Series in Optical Sciences, vol. 232.
Springer, Cham, 522 p. 2020. –Available
at: <https://doi.org/10.1007/978-3-030-45700-6>,(2020). DOI:10.1007/
978-3-030-45700-6.

[17] Gerd Keiser, Optical Fiber
Communications, McGraw Hill, 4th
edition, 2008.

[18] Prajwalasimha S. N., Kamalesh V. N.
Macro Bending Loss in Single Mode
Optical Fibre Cable for Long Haul
Optical Networks, International Journal
of Emerging Technology and Advanced
Engineering, Volume 4, Issue 6, June,
2014.

IntechOpen